ELSEVIER

Journal of Power Sources 54 (1995) 338–341

JOURNAL OF POWER SOURCES

Charge and discharge characteristics of lithium-ion graphite electrodes in solid-state cells

S. Lemont, D. Billaud

Laboratoire de Chimie Minérale Appliquée, URA CNRS No. 158, BP 239, Université de Nancy I, Vandoeuvre-les-Nancy Cedex, France

Abstract

Lithium ions have been electrochemically intercalated into graphite in solid-state cells operating with solid polymer electrolytes based on poly(ethylene oxide) (PEO) complexed with lithium perchlorate ($LiClO_4$). The working composite electrode is composed of active-divided natural graphite associated with $P(EO)_8$–$LiClO_4$ acting as a binder and a Li^+ ionic conductor. Intercalation and de-intercalation of Li^+ were performed using galvanostatic or voltammetry techniques. The curves obtained in our solid-state cells were compared with those performed in liquid ethylene carbonate–$LiClO_4$ electrolyte. It is shown that in solid-state cells, side reactions occur both in the reduction and in the oxidation processes which leads to some uncertainty in the determination of the maximum reversible capacity of the graphite material.

Keywords: Graphite; Lithium-ion batteries; Solid-state cells

1. Introduction

Much effort has been devoted to the development of solid-state rechargeable lithium batteries operating with polymer electrolytes [1–5]. Such power sources offer high energy density but suffer from loss of capacity on cycling. This represents a major obstacle in the development of these batteries. The limited rechargeability and the safety hazards of Li anode batteries can be overcome with the use of materials with lower Li activity in the anode than metallic lithium. It is expected that a lower activity will reduce the risk of anode passivation. Among the possible alternative anodes, lithium-graphitized carbon intercalation compounds appear to be suitable [2]. It is believed that graphite has a theoretical intercalation capacity of 1 Li per 6 C, according to the equation $Li + 6C = LiC_6$. However, several parameters affect the reversible Li intercalation efficiency of carbon: crystallinity, texture, and nature of the surface groups. Some of our recent investigations on the behaviour of different graphitic materials cycled in liquid electrolytes have shown that the maximum capacity x (x refers to Li_xC_6) was strongly dependent on the morphology of the graphitic electrode and on the electrolyte composition; solutions composed of ethylene carbonate (EC) and $LiClO_4$ or $LiBF_4$ as conducting salts appeared very suitable to obtain the intercalation of unsolvated Li^+ up to the maximum LiC_6 capacity [6–9]. We have also studied, for comparison, the Li^+ intercalation into graphite using all-solid-state cells operated with a solid polymeric electrolyte based on poly(ethylene oxide) (PEO), and lithium perchlorate, $LiClO_4$ [10]. More extensive data are given in this paper.

2. Experimental

The button-type cells used in this study are composed of an Li electrode, a complex of PEO and $LiClO_4$, $P(EO)_8LiClO_4$, acting as solid polymeric electrolyte and a composite electrode containing both fine graphite powder UF_4 (Le Carbone Lorraine, France) as the active material and the electrolyte as a binder. The electrolyte was prepared by solving both PEO (average mol. wt. 5×10^6, Aldrich) and $LiClO_4$ (Aldrich) into acetonitrile in a molar ratio PEO:Li = 8:1. This solution was then poured on to a Teflon plate and the solvent was evaporated up to the formation of a polymeric conducting film which is finally dried at 80 °C under vacuum. The composite electrode was prepared by stirring graphite UF_4, previously outgassed at 600 °C under secondary vacuum, with the electrolytic acetonitrile solution described above. This heterogeneous solution was cast on to a side of the button cell, then vacuum heated at around 120 °C for several hours.

SSDI 0378-7753(94)02096-L

$LiClO_4$ was dried at 180 °C under secondary vacuum before utilization and acetonitrile was dried over $CaCl_2$ and distilled by cryogenic pumping. The solid-state cell was operated at 80 °C to insure a high ionic conductivity of the electrolyte [11]. Electrochemical studies were conducted with a PAR 273 potentiostat/galvanostat working either in galvanostatic or voltammetry modes. A computer-controlled multichannel Mac Pile potentiostat/galvanostat was also used to obtain curves in pulse charge or discharge mode [12].

3. Results and discussion

Fig. 1 shows the evolution of the cell voltage versus Li^+/Li^0 during a constant charge/discharge cycle for the system $Li/P(EO)_8LiClO_4/graphite(UF_4)–P(EO)_8$-$LiClO_4$. In the composite electrode, the weight ratio graphite:PEO is equal to 55:45. The experiment is carried out at 83 °C with an electrolysis current of 1.49 μA/mg. These curves present potential slopes and plateaus typical of pure phase stoichiometric domains and biphasic systems, respectively. The shapes of these curves with the ones recently obtained during the Li^+ intercalation into graphite in a liquid EC–$LiClO_4$ electrolyte and the different phases (intercalation stages) formed during the charge/discharge process have been characterized by X-ray diffraction studies [6,7]. The compound obtained near 0 V versus Li^+/Li is the well-known golden LiC_6 stage I. However, a coulombmetric titration for the charge curve of Fig. 1 demonstrates that only 24 wt.% of the graphite is intercalated, assuming an LiC_6 composition. Such a low yield was attributed to the inhomogeneous distribution of graphite in the composite electrode. An important part of graphite particles can be electrically isolated from the metallic electron collector. Fig. 2 related to the ninth charge/discharge cycle of the previous cell is comparable with Fig. 1. It must be noticed, however, that the potential plateaus tend to disappear as if Li^+ intercalation and de-intercalation do not proceed anymore via successive

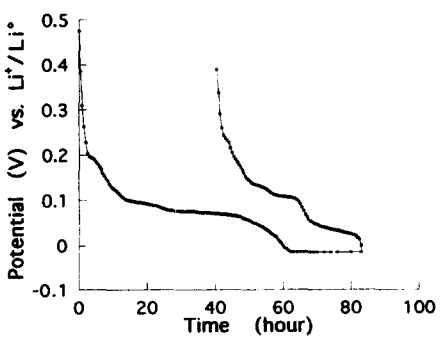

Fig. 1. Constant-current charge and discharge curves at 1.49 μA/mg of the $Li/P(EO)_8LiClO_4/UF_4–P(EO)_8LiClO_4$ system (55 wt.% UF_4).

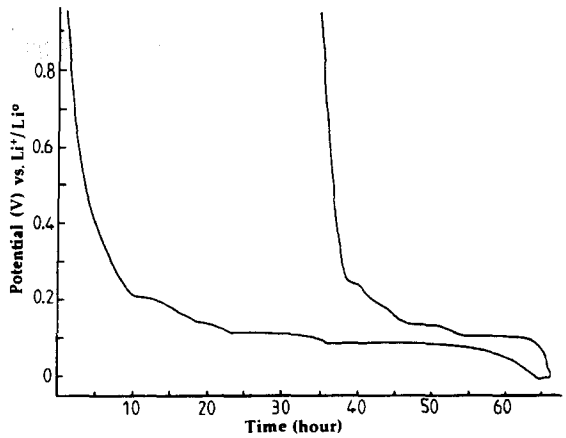

Fig. 2. Ninth charge/discharge cycle of the same system presented in Fig. 1.

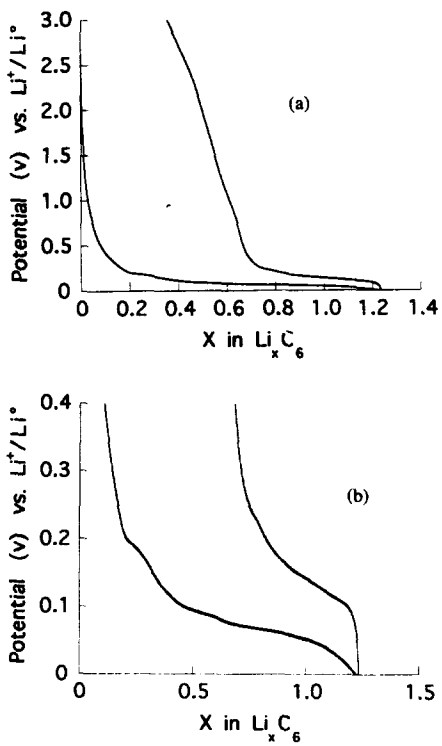

Fig. 3. (a) Fourth constant-current charge/discharge curve at 10 μA of UF_4, 0.230 mg (65 wt.% UF_4). (b) Enlarged scale charge/discharge curve of Fig. 3(a) between 0.4 and 0 V.

well-defined stages. This could be related to kinetic problems due to side reactions which can affect the diffusion of Li^+ or electrons through the interface between the graphite particles and the PEO complex.

Fig. 3 presents the fourth charge/discharge cycle at 80 °C and conducted using the Mac Pile potentiostat/galvanostat between 3 and 0 V. The composite electrode contains 0.230 mg of graphite UF_4 and the weight ratio graphite:PEO is here equal to 65:35. The electrolysis current is equal to 10 μA. The cell is allowed to relax for 0.017 h if the cell potential variation is higher than

50 mV. Fig. 3(b) shows the same charge/discharge curve with an enlarged scale between 0.4 and 0 V. It appears that the apparent charge capacity x (x refers to Li_xC_6) at 0 V is equal to 1.22, much higher than the theoretical $x=1$ in LiC_6. In fact, large differences appear in the shapes of the charge curves obtained in our solid-state cells and those performed in liquid EC–$LiClO_4$ electrolytes [7,9]. In the latter, the initial potential decreases very sharply from 3 to around 0.25 V which corresponds to a plateau identified as the dilute stage I/stage IV transformation. The beginning of this plateau occurs for x close to 0.07. To the contrary, the beginning of this plateau corresponds in Fig. 3(b) to $x=0.2$. It is clear that such differences in x values are related to side reactions occurring during the charge (reduction) process. The discharge (oxidation) curve up to 3 V corresponds to $\Delta x=0.893$ while the discharge up to 0.7 V gives $\Delta x=0.576$. Here also, differences appear with the experiments obtained in liquid electrolyte cells. The increase of the potential from 0.25 to 3 V occurs in the x range 0.7–0.33, when the oxidation wave is carried out in a solid-state cell. In reactions performed in liquid electrolyte, the corresponding variation of the potential values occur in a Δx range equal to 0.05. The convexity of the corresponding parts of these discharge curves are also different. The side reactions which occur during the beginning of the charge process of a composite electrode containing 69 wt.% of graphite can be evidenced in Fig. 4 obtained during the first charge of graphite UF_4 (0.524 mg); an intensity of -2.5 μA is applied to the cell. The two breaks which appear in the curve at 1.5 and at 0.8 V are extended between $x=0$ and $x=0.2$, respectively. Over this last value, the intercalation curve is similar to that is found when the experiments are carried out in EC–$LiClO_4$ electrolyte. The voltammogram presented in Fig. 5 gives also evidence for side reactions occurring both in the reduction and the oxidation process (first cycle). Such a voltammogram has been obtained from a composite electrode composed of natural Ceylon graphite (200 μm, 67 wt.%), $P(OE)_8LiClO_4$ complex (19 wt.%) and carbon black (14 wt.%). The sweep rate is equal to 4×10^{-3} mV

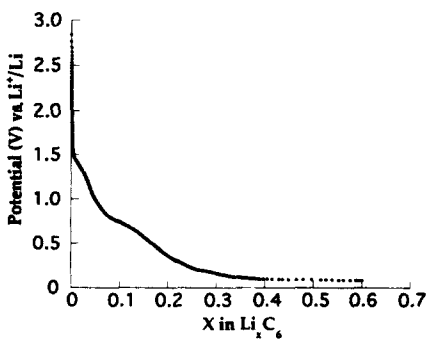

Fig. 4. First charge curve at 2.5 μA of graphite UF_4, 0.524 mg (69 wt.% UF_4).

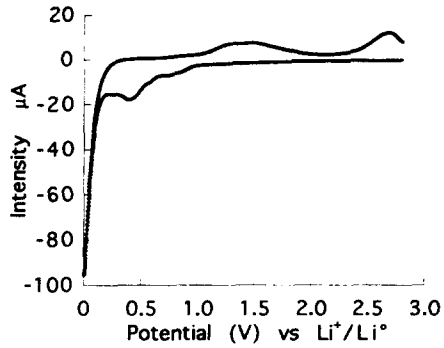

Fig. 5. First cyclic voltammogram of the Li/$P(EO)_8LiClO_4$/graphite (67 wt.%)–carbon black (14 wt.%)–electrolyte (19 wt.%) system; sweep rate $=4\times10^{-3}$ mV/s.

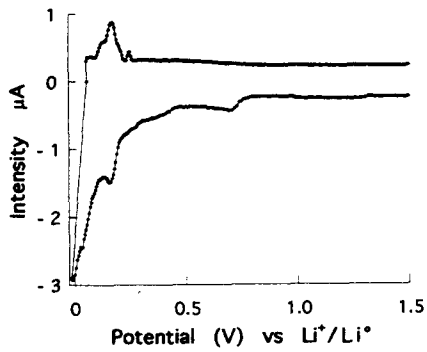

Fig. 6. Second voltammogram carried out after the fourth cycle presented in Fig. 3(a); sweep rate = 10 mV/h.

s^{-1}. During the reduction process, a cathodic current appears from around 1 to 0.200 V where the intercalation starts: two broad peaks centred around 0.9 and 0.4 V are apparent. In the oxidation waves, two important peaks appear at 1.5 and 2.7 V but no peak occurs at 0.8 V. The origins of these side reactions occurring either in reduction or in oxidation processes are still unclear and they influence the value of the apparent reversible capacity of the cell. Extra experiments are needed with different solid electrolytes–graphitized carbon associations in order to shed more light on these side reactions.

Fig. 6 presents a second voltammogram carried out between 1 and -0.015 V after the fourth charge/discharge cycle presented in Fig. 3(a). The potential scan rate is equal to 10 mV/h. In the reduction process, the very extended peak appearing between 0.75 an 0.5 V is still present, due to side reactions. The peaks related to Li^+ intercalation are noticeable from 0.25 up to -0.015 V. In the oxidation wave, only the expected de-intercalation peaks are visible at 0.12, 0.187 and 0.246 V.

4. Conclusions

Lithium ions can be intercalated into graphite in solid-state cells operating with a polymer electrolyte

such as $P(EO)_8LiClO_4$. However, due to kinetic problems, inhomogeneous intercalated compounds composed of different intercalation stages and sometimes of pure graphite are usually obtained even for very low intercalation rates. Such problems can be partially overcome by using composite working electrodes composed of graphite as active material and of a binder, which is also an Li^+-ion conductor, such as $P(EO)_8LiClO_4$. In these conditions, the pure-metal-rich LiC_6 stage-I intercalation compound can be obtained by application of suitable electrolysis current densities or at moderated potential scan rates in order to avoid metal lithium deposition. The electrochemical capacity x (x refers to Li_xC_6 compound) found in some of our experiments is higher than 1 which is an evidence for side reactions which occur before the beginning of the intercalation reaction. In the de-intercalation process, side reactions appear also around 0.5 and 2.7 V. These side reactions are not only related to the polymer electrolyte but also to graphite since similar Li^+ intercalation into fullerene, which leads to only three reversible intercalation transformations in the potential range from 1.1 to 2.7 V versus Li^+/Li, does not give evidence for such side reactions [10,13]. Their origin must be cleared by characterizing the different side products which are formed besides the Li_xC_6 intercalation compounds. Such studies using analytical transmission electron microscopy are now in progress.

References

[1] M.B. Armand, J.M. Chabagno and M.J. Duclot, in P. Vashista, J.N. Mundy and G.K. Shenoy (eds.), *Fast Ion Transport in Solids*, Elsevier, Amsterdam, 1979, p. 131.

[2] M.B. Armand, in D.W. Murphy, J. Broadhead and B.C. Steele (eds.), *Material for Advanced Batteries*, Plenum, New York, 1980, p. 145.

[3] J.S. Lundsgaard, S. Yde-Andersen, R. Koksbang, D.R.Shackle, R.A. Austin and D. Fauteaux, in B. Scrosati (ed.), *Proc. 2nd Int. Symp. Polymer Electrolytes, Sienna, Italy*, Elsevier Applied Science, Barking, UK, 1990, p. 395.

[4] S. Kato, Y. Yoshihisa, K. Takeuchi and K. Murata, in T. Keily and B.W. Baxter (eds.), *Power Sources 13, Proc. 17th Int. Power Sources Symp., Bournemouth, UK, 1991*, p. 409.

[5] K.M. Abraham, *Electrochim. Acta, 38* (1993) 1233.

[6] D. Billaud, F.X. Henry and P. Willmann, *Mater. Res. Bull., 28* (1993) 477.

[7] D. Billaud, F.X. Henry and P. Willmann, *Mol. Cryst. Liq. Cryst., 245* (1994) 159.

[8] P. Willmann, D. Billaud and F.X. Henry, *Proc. European Space Power Conf., Graz, Austria, 1993*, p. 789.

[9] D. Billaud, F.X. Henry and P. Willmann, *J. Power Sources, 54* (1995) 383.

[10] S. Lemont, J. Ghanbaja and D. Billaud, *Mol. Cryst. Liq. Cryst., 244* (1994) 203.

[11] M.B. Armand, *Polym. Electrolyte Rev., 1* (1987) 1.

[12] C. Mouget and Y. Chabre, *Multichannel Potentiostat Galvanostat 'Mac Pile'*, licensed from CNRS and UJF Grenoble to Bio-Logic, Claix, France.

[13] Y. Chabre, D. Djurado, M. Armand, W.R. Romanov, N. Coustel, J.P. Mc Cauley, J.E. Fischer and A. Smith, *J. Am. Chem. Soc., 114* (1992) 764.